BIOCHEMISTRY
including biophysical chemistry & molecular biology

Article

pubs.acs.org/biochemistry

Kinetic Analysis of the Unique Error Signature of Human DNA Polymerase ν

Mercedes E. Arana,[†] Olga Potapova,[‡] Thomas A. Kunkel,[†] and Catherine M. Joyce*[,‡]

[†]Laboratory of Molecular Genetics and Laboratory of Structural Biology, National Institute of Environmental Health Sciences, National Institutes of Health, Department of Health and Human Services, Research Triangle Park, North Carolina 27709, United States

[‡]Department of Molecular Biophysics and Biochemistry, Yale University, New Haven, Connecticut 06520, United States

Supporting Information

ABSTRACT: The fidelity of DNA synthesis by A-family DNA polymerases ranges from very accurate for bacterial, bacteriophage, and mitochondrial family members to very low for certain eukaryotic homologues. The latter include DNA polymerase ν (Pol ν) which, among all A-family polymerases, is uniquely prone to misincorporating dTTP opposite template G in a highly sequence-dependent manner. Here we present a kinetic analysis of this unusual error specificity, in four different sequence contexts and in comparison to Pol ν's more accurate A-family homologue, the Klenow fragment of *Escherichia coli* DNA polymerase I. The kinetic data strongly correlate with rates of stable misincorporation during gap-filling DNA synthesis. The lower fidelity of Pol ν compared to that of Klenow fragment can be attributed primarily to a much lower catalytic efficiency for correct dNTP incorporation, whereas both enzymes have similar kinetic parameters for G-dTTP misinsertion. The major contributor to sequence-dependent differences in Pol ν error rates is the reaction rate, k_{pol}. In the sequence context where fidelity is highest, k_{pol} for correct G-dCTP incorporation by Pol ν is ~15-fold faster than k_{pol} for G-dTTP misinsertion. However, in sequence contexts where the error rate is higher, k_{pol} is the same for both correct and mismatched dNTPs, implying that the transition state does not provide additional discrimination against misinsertion. The results suggest that Pol ν may be fine-tuned to function when high enzyme activity is not a priority and may even be disadvantageous and that the relaxed active-site specificity toward the G-dTTP mispair may be associated with its cellular function(s).

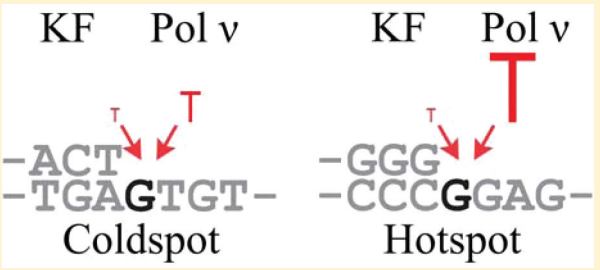

Cells rely on a variety of processes to ensure faithful DNA replication and repair, and DNA polymerases play key roles in these processes. The human genome encodes at least 15 DNA polymerases (reviewed in ref 1). Three of these enzymes, DNA polymerases γ (Pol γ), θ (Pol θ), and ν (Pol ν), are members of the A-family of DNA polymerases because they share homology with *Escherichia coli* DNA polymerase I, encoded by the *polA* gene. The focus of this study is Pol ν, encoded by the human *POLN* gene.[2] Although the biological role of Pol ν is uncertain, one clue about its possible function is its homology to *Drosophila melanogaster* Mus308, an A-family DNA polymerase with a helicase domain at the N-terminus.[3] *Mus308* mutants are hypersensitive to DNA cross-linking agents (nitrogen mustard and cisplatin) but not to MMS,[4] implicating Mus308 in the repair of highly toxic interstrand cross-links.[2,4,5] *POLN*-knockdown cells are sensitive to various DNA-damaging agents,[6,7] including DNA cross-linking agents, indicating that Pol ν may be involved in repairing lesions generated by these agents. There is also functional and physical evidence of the interaction of Pol ν with proteins involved in the Fanconi-anemia pathway that is involved in repair of cross-linked DNA.[7] Consistent with possible roles in cross-link repair, Pol ν can bypass a psoralen DNA interstrand cross-link[6] and DNA interstrand cross-links with linkages through the DNA major groove.[8] It can also bypass a subclass of thymine glycol lesions.[9] Pol ν is a processive enzyme and performs efficient strand-displacement synthesis, and these properties may be important for its biological function.

Several A-family DNA polymerases, including *E. coli* Pol I,[10] T7 DNA polymerase,[11,12] and Pol γ,[13−15] have intrinsic 3′ to 5′ exonuclease activity that can edit the occasional mismatches they create, thereby enhancing the fidelity with which they synthesize DNA.[16,17] Other A-family DNA polymerases, such as *Taq* DNA polymerase[18,19] and *Bst* DNA polymerase,[20] lack intrinsic 3′ to 5′ exonuclease activity and therefore cannot proofread their mistakes. Nonetheless, they are among the most accurate of the naturally exonuclease-deficient polymerases.[18−23] Pol θ and Pol ν comprise yet a third subtype of A-family polymerase. They too lack 3′ to 5′ exonuclease activity, but they have low nucleotide selectivity. For example, compared to the exonuclease-deficient form of the Klenow fragment of *E. coli* Pol I, human Pol θ has a much lower

Received: August 2, 2011
Revised: October 17, 2011
Published: October 18, 2011

selectivity and forms a variety of different single-base mismatches at high rates.[24] Human Pol ν also has low nucleotide selectivity, but its specificity is much more biased, specifically for misinsertion[9] and stable misincorporation of dTTP opposite template G.[25] Moreover, when stable misincorporation of dTTP was monitored opposite a large number of template guanines, the site-to-site variation in the error rate for the G-dTTP mismatch was more than 30-fold.[25]

Previous studies of error specificity have provided clues about the biological functions of DNA polymerases. For example, studies of the error specificity of human Pol η[26] eventually led to the conclusion that it is responsible for base substitutions at A-T base pairs during somatic hypermutation of immunoglobulin genes.[27−29] Also, studies of the error specificity of yeast replicases[30−32] have led to a better understanding of leading and lagging strand DNA replication in vivo. It is our hope that the unusual error specificity of human Pol ν will likewise result in a better understanding of its biological function(s). In this study, we have focused particularly on the sequence dependence of misincorporation, a well-documented phenomenon that remains poorly understood. Pol ν's preference for forming G-dTTP mispairs in a highly sequence-dependent manner allowed us to investigate the kinetic parameters for correct and incorrect dNTP insertion and mismatch extension at hotspots and coldspots. Examining the kinetic parameters for correct and incorrect dNTP insertion by Pol ν in four different sequence contexts, we have found that the error rate for stable misincorporation of dTTP opposite template G correlates strongly with the kinetic parameters for correct dNTP insertion, as has been previously noted for a variety of DNA polymerases.[33,34]

EXPERIMENTAL PROCEDURES

Enzymes, Reagents, DNA Oligonucleotides. Materials for the M13mp2 fidelity assay were from sources described previously.[35] Ultrapure dNTPs were purchased from Amersham Biosciences (GE Healthcare). Pol ν fragment 1 (E175−G863, 77.1 kDa, Pol ν-77) was expressed and purified as previously described.[9,36] Exonuclease-deficient (D424A) Klenow fragment was purified according to our published procedures.[37,38] DNA oligonucleotides were synthesized by the Keck Biotechnology Resource Laboratory at Yale University Medical School and were purified by denaturing gel electrophoresis as described previously.[39]

M13mp2 Fidelity Assay. The fidelity assay scores errors generated in the *lacZ* α-complementation gene in M13mp2 during synthesis to fill a 407-nucleotide gap. Reaction mixtures (25 μL) to fill the gap contained 0.2 nM M13mp2 gapped DNA substrate, 20 mM Tris-HCl (pH 7.5 or 8.8), 8 mM $Mg(OAc)_2$, 2 mM DTT, 80 μg/mL of bovine serum albumin, 4% (v/v) glycerol, and dATP, dGTP, dCTP, and dTTP (1 mM each). Reactions were initiated by addition of Pol ν-77 (200 nM), incubated at 37 °C for 30 min, and terminated by addition of EDTA to a final concentration of 20 mM. Half of the reaction mixture was mixed with SDS buffer [20 mM Tris-HCl (pH 8.0), 5 mM EDTA, 5% SDS, 0.5% bromophenol blue, and 20% glycerol] and analyzed by agarose gel electrophoresis. The results indicated that the gap was completely filled for reactions performed at both pH values (data not shown, but for a typical result, see ref 25). Aliquots of the remaining DNA products were then used to determine *lacZ* mutant frequencies for the purpose of obtaining error rates, as described previously.[25] Correct synthesis produces M13mp2 DNA that yields dark blue M13 plaques when introduced into an *E. coli* α-complementation strain and plated on indicator plates. Polymerase errors are scored as light blue or colorless M13 plaques. DNA from independent mutant clones was sequenced to define the sequence changes in *lacZ*, and this information was used to calculate error rates as described in ref 35. Error rates for individual types of mutation were calculated according to the equation $ER = [(N_i/N)MF]/(0.6D)$, where N_i is the number of mutations of a particular type, N is the total number of mutants analyzed, MF is the frequency of *lacZ* mutants, D is the number of detectable sites for the particular type of mutation, and 0.6 is the probability of expressing a mutant *lacZ* allele in *E. coli*.[35]

Chemical Quench Kinetic Measurements. Table 1 lists the sequences of the duplex DNA substrates used in this study.

Table 1. DNA Duplex Oligonucleotides Used in Kinetic Experiments

Name	DNA sequence
Misinsertion substrates	
13/19mer-G	5′GAGTCAACAGGTC 3′CTCAGTTGTCCAG**G**TATGG
13/19mer-T	5′GAGTCAACAGGTC 3′CTCAGTTGTCCAG**T**GATGG
G(165) hotspot	5′GCGATCGGTGCGGG 3′CGCTAGCCACGCCC**G**GAGAAGCGA
G(164) hotspot	5′GCGATCGGTGCGGGC 3′CGCTAGCCACGCCCG**G**AGAAGCGA
G(-66) coldspot	5′TGAGTGAGCTAACT 3′ACTCACTCGATTGA**G**TGTAATTAA
Mismatch extension substrates (X = C or T)	
14/19mer-G	5′GAGTCAACAGGTC**X** 3′CTCAGTTGTCCAG**G**TATGG
G(165) hotspot	5′GCGATCGGTGCGGG**X** 3′CGCTAGCCACGCCC**G**GAGAAGCGA
G(-66) coldspot	5′TGAGTGAGCTAACT**X** 3′ACTCACTCGATTGA**G**TGTAATTAA

Primer strands, 5′-labeled with ^{32}P, were annealed to a 1.5-fold molar excess of the appropriate template strand. Primer extension reactions were conducted at room temperature (20−22 °C) using a rapid-quench-flow instrument (KinTek Corp., model RQF-3) for fast reactions and manual quenching when the reaction was sufficiently slow. In either case, the reaction was initiated by mixing equal volumes of a polymerase/DNA mix and a dNTP solution, both in Pol ν reaction buffer [20 mM Tris-HCl (pH 7.5), 8 mM $Mg(OAc)_2$, 2 mM DTT, 4% (v/v) glycerol, and 80 μg/mL bovine serum albumin]. The final reaction mixture contained 5 nM primer−template duplex, 7 nM Pol ν-77, and varying dNTP concentrations. The preparation of Pol ν-77 used in the majority of the kinetics measurements was ∼23% active, and therefore the concentrations listed above gave burst kinetics[40,41] with a burst amplitude of ∼0.3. Reactions were quenched at appropriate time intervals using excess EDTA, and

Table 2. Summary of Sequence Changes Generated by Pol ν-77

	pH 7.5[a]		pH 8.8[b]	
lacZ mutant frequency	0.035		0.15	
total no. of mutants sequenced	204		152	
total no. of bases sequenced	83028		61864	
detectable changes[c]	no. of changes	error rate ($\times 10^{-4}$)	no. of changes	error rate ($\times 10^{-4}$)
base substitutions	204	4.7	227	30
frameshifts (−1)	16	0.23	15	1.2
frameshifts (+1)	10	0.14	7	0.6
G·dTTP	168	22.0	190	150
T·dGTP	19	2.0	17	10

[a]Error rates and mutant frequencies. In experiment 1, the mutant frequency was 2.1% (47 mutant plaques from a total of 2240) and, in experiment 2, the mutant frequency was 4.8% (192 mutant plaques from a total of 3994). [b]Error rates and mutant frequencies were calculated using data from three independent experiments. In experiment 1, the mutant frequency was 16.0% (484 mutant plaques from a total of 2947). In experiment 2, the mutant frequency was 15% (581 mutant plaques from a total of 3771). In experiment 3, the mutant frequency was 13% (783 mutant plaques from a total of 5927). [c]Error rates calculated from detectable changes (ref 35 and see Experimental Procedures). The total number of specific mutations reported is greater than the number of *lacZ* mutants sequenced because of the presence of >1 detectable errors in certain mutants.

mixtures were fractionated on denaturing polyacrylamide−urea gels and quantitated on a Fuji FLA 5100 scanner. The fraction of labeled DNA converted to product was plotted as a function of reaction time and fitted to the burst relationship:

$$A[1 - \exp(-k_{obs}t)] + k_{ss}t$$

Burst rate constants (k_{obs}, corresponding to the rate constant for the first turnover) were determined at a series of dNTP concentrations, and k_{pol} and K_d were determined from a plot of k_{obs} versus dNTP concentration fitted to the hyperbolic equation $k_{obs} = k_{pol}[dNTP]/(K_d + [dNTP])$. In a few instances, where a lack of sufficient Pol ν precluded use of the rapid-quench instrument, rate measurements were made at very low dNTP concentrations using manual quenching. At low dNTP concentrations, the hyperbolic equation is reduced to $k_{obs} = k_{pol}[dNTP]/K_d$, allowing the ratio k_{pol}/K_d to be obtained directly from the slope of the plot of k_{obs} versus dNTP concentration.

Gel Mobility Shift Studies of DNA Binding. Pol ν-77, at a series of concentrations from 0.05 to 100 nM, was incubated with ^{32}P-labeled duplex DNA in Pol ν reaction buffer, with an additional 10% glycerol, for 10 min at 22 °C. The samples were loaded onto an 8% polyacrylamide gel, poured and run in 50 mM Tris borate, 2 mM $MgCl_2$, and 0.1 mM EDTA. The samples were loaded with the gel running at 300 V, and then electrophoresis was continued at 150 V for 3−4 h at 4 °C. The gel was dried down, and radioactivity was quantitated on a Fuji FLA 5100 scanner. Two types of information were obtained from plots of the fraction of bound DNA as a function of the concentration of Pol ν-77, as illustrated in Figure S1 of the Supporting Information. With 1 nM DNA, which is greater than the K_D, the fraction of DNA bound to Pol ν-77 is given by $f[Pol]/[DNA]$, so that the slope of the graph allowed us to determine f, the fraction of the added Pol ν-77 that is active in binding DNA. At a DNA concentration below K_D, the fraction of bound DNA approximates the hyperbolic relationship $[Pol]/([Pol] + K_D)$, allowing calculation of K_D.

RESULTS

Error Specificity. Our earlier study highlighted the tendency of full-length human Pol ν to generate G to A substitutions via misincorporation of dTTP opposite template guanine.[25] We began this study by confirming this error signature for a slightly abbreviated derivative of Pol ν (the eventual goal being structural studies), designated Pol ν-77.[36] We used the M13mp2 forward mutation assay, which detects a wide range of sequence changes in the *lacZ* gene in a variety of sequence contexts.[35] The DNA products of gap-filling synthesis at pH 8.8 yielded an average *lacZ* mutant frequency of 15% (Table 2), comparable to the value of 18% reported previously for the full-length protein.[25,36] In addition to similar error rates, the truncated and full-length Pol ν proteins have similar processivity (compare Figure 2 of ref 25 and Figure 4 of ref 36). We also examined the fidelity at pH 7.5, the pH used in our kinetic studies below. Pol ν is more accurate at pH 7.5, as revealed by a 4-fold lower average mutant frequency of 3.5% (Table 2). Higher accuracy at lower pH is also a characteristic of other A-family DNA polymerases, including *Taq* polymerase[19] and the large Klenow fragment of *E. coli* pol I.[42] When 204 independent *lacZ* mutants were sequenced from reactions performed at pH 7.5, a variety of single-base changes were observed (Table 2). These were distributed throughout the *lacZ* target sequence (Figure 1), in a pattern similar to that seen earlier with full-length human Pol ν at pH 8.8.[25] Substitutions predominated, and the vast majority were G to A changes, yielding an average error rate of 22×10^{-4} for stable misincorporation of dTTP opposite the 22 template guanines where this event results in a change in plaque color.[35] The second most common error was the mismatch involving the same two bases but differing with respect to the templating versus incoming base, i.e., the T-dGTP mismatch [average error rate of 2.0×10^{-4} (Table 2)]. We have previously compared Pol ν specific error rates to the error rates of other DNA polymerases (see Table 2 of ref 25).

As described previously,[25] G to A mutation rates varied by sequence context. The highest mutation rate for a phenotypically detectable site was observed at template guanine +165 [designated the G(165) hotspot], where 38 substitutions were observed among 204 sequenced *lacZ* mutants. This corresponds to an error rate of 1.1%; because of this high error rate, the G(165) hotspot sequence was chosen for our kinetic analysis. Additionally, we measured dNTP insertion kinetics at the neighboring guanine, G(164), which is also a hotspot. Although substitutions at G(164) are phenotypically silent, two G to A substitutions were observed as silent hitchhikers among 204 sequenced *lacZ* mutants, corresponding to an error rate of 1.6%, similar to the error rate at G(165).[a] For comparison, we

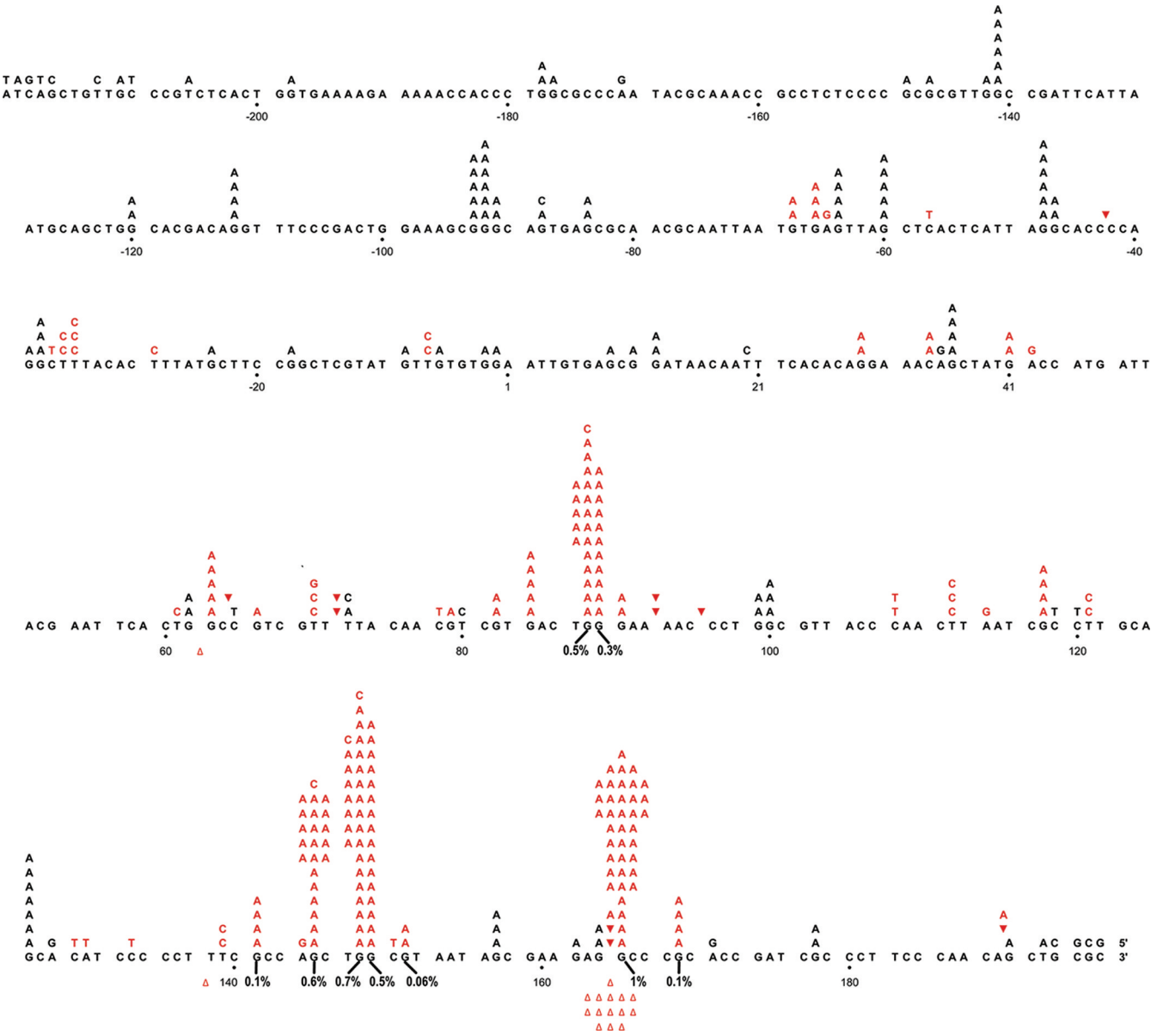

Figure 1. Spectrum of errors generated by human Pol ν-77 at pH 7.5. The 407 template nucleotides within the single-strand gap of the M13mp2 substrate are shown as five lines of the template sequence, bracketed by 5 bp at either end to indicate the boundaries of the gap; +1 represents the first transcribed nucleotide of the *lacZα* complementation region. Letters above the target sequence indicate base substitutions made by Pol ν-77. Single-base deletions are denoted by empty triangles below the target sequence, whereas single-base additions are depicted by filled inverted triangles above the target sequence. Red characters represent phenotypically detectable changes in the gap region, while black characters represent phenotypically undetectable changes found in association with detectable changes. Also depicted in the figure are the error rates at positions 88, 89, 141, 145, 148, 149, 151, 165, and 169.

analyzed Pol ν kinetics at a mutational coldspot, G(−66), selected because only three G to A changes were detected at this phenotypically detectable position, corresponding to an error rate of 0.09%.

dNTP Misinsertion. The design of the kinetics experiments was influenced by the properties of the Pol ν-77 preparations. Purification of Pol ν-77 is challenging, and the purified protein[36] was typically not fully active, as shown by active-site titration using the measurement of burst amplitudes in primer extension reactions (Figure 2A,B). An alternative method using DNA binding to assess the concentration of active Pol ν-77 is illustrated in Figure S1 of the Supporting Information. Measurements by the two methods were in good agreement. The Pol ν-77 preparation used in the majority of the kinetics experiments contained 23% active polymerase. As described in Experimental Procedures, we measured reaction rates under burst conditions, with the concentration of active Pol ν-77 being ~3-fold lower than the concentration of the DNA substrate. This had the advantage of conserving our stocks of enzyme and also avoided the problem that high concentrations of some Pol ν-77 preparations inhibited the reaction.

We measured misinsertion by Pol ν-77 on several different DNA substrates (Table 1). The 13/19mer duplex is a DNA substrate that we have used routinely in recent kinetic studies of Klenow fragment.[38,43] We compared misinsertions at a template T and a template G in this sequence. The results with Klenow fragment (Table 3, line 2 of each section) were in

dx.doi.org/10.1021/bi201197p | *Biochemistry* 2011, 50, 10126–10135

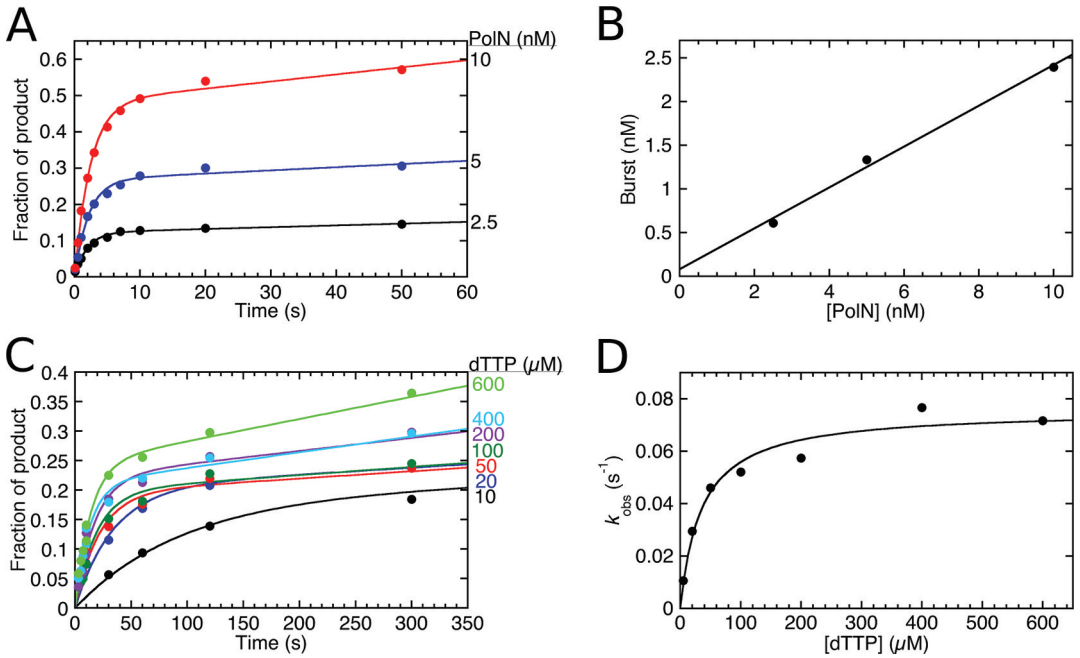

Figure 2. Kinetics of Pol ν-77. (A) Kinetics of incorporation of dATP into the 13/19mer-T substrate (Table 1). The reaction mixtures contained 5 nM DNA primer termini, 100 μM dATP and the indicated concentrations of Pol ν-77 (measured as total protein). Because the Pol ν-77 preparation was not fully active, all three concentrations of Pol ν-77 showed burst kinetics, with the burst amplitude providing a measure of the concentration of the active enzyme. (B) The plot of burst amplitude vs Pol ν-77 concentration has a slope of 0.23, indicating that this Pol ν-77 preparation was 23% active. (C) dTTP misinsertion by Pol ν-77 opposite template G within the G164 hotspot sequence, measured under burst conditions at a series of dTTP concentrations. (D) Burst rate constant for G-dTTP misinsertion plotted as a function of dTTP concentration and fitted to a hyperbolic equation, giving $K_{d(dTTP)}$ of 35 μM and k_{pol} of 0.076 s^{-1}.

good agreement with data previously obtained on a different DNA sequence (reproduced in Table 3, line 1 of each section).[44] As described above, three other DNA substrates were derived from the *lacZ* target sequence, to study dTTP misinsertion opposite template guanines in three different sequence contexts: the G(164) and G(165) hotspots and the G(−66) coldspot. In each case, we measured the rates of correct and mismatched dNTP incorporation at a series of dNTP concentrations and calculated k_{pol} and $K_{D(dNTP)}$. Panels C and D of Figure 2 show an example of the data obtained for T misinsertion opposite G(164). The misinsertion data obtained for Pol ν-77, with selected Klenow fragment misinsertions for comparison, are listed in Table 3. The final column of Table 3 compares the efficiencies of correct and incorrect dNTP addition on each substrate, giving the selectivity in favor of the correct complementary dNTP.

The misinsertion data for the 13/19mer substrate fit well with the overall mutational data for both Klenow fragment and Pol ν. For example, Klenow fragment has 3-fold weaker discrimination against T-dGTP errors [1.3×10^{-4} (bottom of Table 3)] compared to G-dTTP errors [3.4×10^{-4} (top of Table 3)], consistent with its higher G-dTTP error rate in the M13mp2 forward mutation assay.[10] For both T-dGTP and G-dTTP errors, the individual kinetic constants for Klenow fragment show that the selectivity in favor of the correct base pair is made up of ~10-fold discrimination in dNTP binding and ~10^3-fold discrimination in the rate of misincorporation, with the kinetic differences between correctly paired and mispaired substrates slightly larger in the case of G-dTTP errors. For Pol ν, the most frequent error in the M13mp2 assay is G-dTTP, whose rate is 11-fold higher than that of T-dGTP (Table 2). Again, this is reflected in the kinetic data, where we observe a 13-fold difference in discrimination against the two mismatches [selectivity values of 38 for G-dTTP and 510 for T-dGTP (third rows in top and bottom sections of Table 3)].

What accounts for the low fidelity of Pol ν for G-dTTP errors? Both Klenow fragment and Pol ν have similar kinetic constants for misinsertion of dTTP opposite template G (Table 3, top right). However, correct dCTP insertion by Pol ν opposite template G is ~10^3-fold less efficient than correct dCTP insertion catalyzed by Klenow fragment (Table 3, top left). The difference in the efficiency of correct incorporation therefore translates directly to ~10^3-fold lower selectivity of Pol ν against G-dTTP mismatches, compared with Klenow fragment. By contrast, at template T, dGTP misinsertion by Pol ν is ~260-fold less efficient than that of Klenow fragment (Table 3, bottom right, compare 950 vs 3.7). This difference moderates the effect of the large (6300-fold) difference in the efficiency of correct (T-dATP) incorporation (Table 3, bottom left, compare 1.2×10^7 to 1.9×10^3), resulting in ~24-fold lower selectivity of Pol ν against T-dGTP errors.

The kinetic data for G-dTTP misinsertion by Pol ν on the *lacZ* sequences also parallel the mutational data. Error rates in the M13mp2 fidelity assay are high at template G(165) and G(164) and lower at template G(−66). Likewise, selectivity against dTTP misinsertion (Table 3) is at least 20-fold higher opposite template G(−66) (selectivity factor of 520) than opposite templates G(165) and G(164) (selectivity factors of 22 and 25, respectively). The different selectivity values derive from some very interesting sequence-dependent differences in individual kinetic constants. First, the binding constants for both correct dCTP and incorrect dTTP are 15−20-fold weaker at the G(−66) position as compared to the G(164) and G(165) positions. At G(−66), where the error rate is lowest,

dx.doi.org/10.1021/bi201197p | *Biochemistry* 2011, 50, 10126–10135

Table 3. Kinetics of dNTP Insertion Catalyzed by Pol ν-77 and by Exonuclease-Deficient Klenow Fragment

	correct dNTP, G·dCTP			incorrect dNTP, G·dTTP			
protein/DNA[a]	K_d (μM)	k_{pol} (s^{-1})	k_{pol}/K_d (M^{-1} s^{-1})	K_d (μM)	k_{pol} (s^{-1})	k_{pol}/K_d (M^{-1} s^{-1})	dC/dT selectivity[b]
Pol I(KF)[c]	8.6	130	1.5×10^7	180	0.03	160	9.4×10^4
Pol I(KF), 13/19mer-G	9.4 ± 0.7	63 ± 7	6.7×10^6	210[d]	0.042[d]	200	3.4×10^4
Pol ν, 13/19mer-G	75 ± 7	0.40 ± 0.003	5.3×10^3	200 ± 15	0.028 ± 0.01	140	38
Pol ν, G(164) hotspot	0.93 ± 0.34	0.057 ± 0.016	6.1×10^4	30 ± 8	0.073 ± 0.005	2.5×10^3	25
Pol ν, G(165) hotspot	1.2 ± 0.3	0.025 ± 0.01	2.1×10^4	24 ± 8	0.022 ± 0.001	940	22
Pol ν, G(−66) coldspot	15 ± 7	0.28 ± 0.004	1.9×10^4	480 ± 140	0.018 ± 0.006	36	520
	correct dNTP, T·dATP			incorrect dNTP, T·dGTP			
protein/DNA[a]	K_d (μM)	k_{pol} (s^{-1})	k_{pol}/K_d (M^{-1} s^{-1})	K_d (μM)	k_{pol} (s^{-1})	k_{pol}/K_d (M^{-1} s^{-1})	dA/dG selectivity[b]
Pol I(KF)[c]	9.1	144	1.6×10^7	48	0.16	3.4×10^3	4.7×10^3
Pol I(KF), 13/19mer-T	8.6 ± 1.0	110 ± 2	1.2×10^7	87 ± 2	0.083 ± 0.01	950	1.3×10^4
Pol ν, 13/19mer-T[e]	–	–	1.9×10^3	140 ± 7	(5.1 ± 0.2) × 10^{-4}	3.7	510

[a]DNA substrates are listed in Table 1. Pol I(KF) is exonuclease-deficient (D424A mutation). Pol ν is the Pol ν-77 fragment. [b]Calculated as $(k_{pol}/K_d)_{correct}/(k_{pol}/K_d)_{incorrect}$. [c]From ref 44, using a different DNA substrate. [d]Single determinations; all others were the average of two or more determinations. [e]$(k_{pol}/K_d)_{correct}$ was determined from the initial slope of the plot of k_{obs} vs dATP concentration, at low dATP concentrations (average of two measurements).

incorporation of correct dCTP is ~16-fold faster than misinsertion of dTTP (Table 3, k_{pol} values of 0.28 and 0.018, respectively). In contrast, at the G(164) and G(165) hotspots, the k_{pol} values for correct dCTP incorporation are slower than that at G(−66) and similar to those for misinsertion of dTTP at these same hotspot sequences. Therefore, the lower fidelity of Pol ν for G-dTTP mismatches in one sequence context as compared to another can be attributed largely to differences in the kinetics of correct G-dCTP incorporation, particularly the rate of dCTP addition, because the ratio of dCTP and dTTP binding constants is very similar at all three sequences. The kinetic constants for the template G in the 13/19mer DNA substrate resemble to some extent those of the G(−66) sequence, with weak binding constants and a fast rate of G-dCTP incorporation.

Mismatch Extension. To examine whether the mispair specificity of Pol ν operates at the level of mismatch extension, we measured the rates of extension of DNA substrates having a terminal (primer)C-G(template) base pair or a T-G mismatch (Table 4). On the 14/19mer extension substrate, both Klenow fragment and Pol ν showed a similar discrimination between C-G and T-G termini, suggesting that mismatch extension does not account for the difference in mutational specificity of these two DNA polymerases. However, the discrimination by Pol ν against extension of the T-G mismatch was modulated by sequence context, with ~8-fold less discrimination at G(165) as compared to G(−66). The difference was primarily due to a faster rate of mispair extension at G(165); the rates of extension of a C-G terminus were similar. Gel mobility shift assays (Figure 3) indicated that binding of Pol ν to the T-G mismatch extension substrates corresponding to the G(165) and G(−66) sequences (Table 1) was indistinguishable (K_D = 0.1 nM, in terms of fully active Pol ν). Therefore, the behavior of Pol ν-77 on the two substrates does not result from a difference in binding affinity. Likewise, there was no difference in the DNA binding behavior of Pol ν upon comparison of the corresponding insertion substrates and C-G extension substrates at the same two sequences (data not shown).

DISCUSSION

Relative to many DNA polymerases that commit T-dGTP errors more frequently than any other base substitution (e.g., Klenow fragment,[10] *E. coli* Pol III,[45] Pol θ,[24] Pol γ,[14,46] Pol η,[26] Pol ι,[47] Pol α,[48] Pol ε,[49] and Pol δ[50]), Pol ν is unusual in preferentially generating a mismatch with the same base composition but the opposite symmetry, i.e., dTTP opposite template G. Not only does Pol ν make this error at much higher rates than for the 11 other single base−base mismatches, it does so in a highly sequence context-dependent manner.[25] The kinetic studies described here examine the binding and rate constants responsible for the unusual properties of Pol ν, in comparison with Klenow fragment, a prototypical A-family polymerase. We first consider results using a common template−primer. We then consider explanations for the site-to-site variations for Pol ν.

T-dGTP versus G-dTTP Errors. A major factor in the low fidelity of Pol ν for both errors is its >10^3-fold lower efficiency of correct dNTP incorporation, compared to that of Klenow fragment, illustrating the general observation that differences in polymerase fidelity are frequently dominated by differences in the kinetics of *correct* base insertion.[33,34] The differences in selectivity of Pol ν and Klenow fragment against particular errors can be understood in terms of the kinetics of the relevant

Table 4. Kinetics of Mismatch Extension Catalyzed by Pol ν-77 and by Exonuclease-Deficient Klenow Fragment

	(primer)C-G			(primer)T-G			
protein/DNA[a]	K_d (μM)	k_{pol} (s^{-1})	k_{pol}/K_d (M^{-1} s^{-1})	K_d (μM)	k_{pol} (s^{-1})	k_{pol}/K_d (M^{-1} s^{-1})	selectivity[b]
Pol I(KF), 14/19mer-G (+dATP)	5.4 ± 1.8	68 ± 14	1.3×10^7	230 ± 60	0.43 ± 0.05	1.8×10^3	6.8×10^3

protein/DNA[a]	k_{obs} (s^{-1}) at 1 mM dNTP	k_{obs} (s^{-1}) at 1 mM dNTP	(CG):(TG) rate
Pol I(KF), 14/19mer-G (+dATP)[c]	68	0.35	190
Pol ν, 14/19mer-G (+dATP)	0.25[d]	$(1.8 \pm 0.2) \times 10^{-3}$	140
Pol ν, G(165) hotspot (+dCTP)	0.16 ± 0.01	$(4.4 \pm 0.6) \times 10^{-3}$	36
Pol ν, G(−66) coldspot (+dATP)	0.22 ± 0.05	$(7.2 \pm 0.7) \times 10^{-4}$	300

[a]Using extension substrates listed in Table 1. [b]Calculated as $(k_{pol}/K_d)_{correct}/(k_{pol}/K_d)_{incorrect}$. [c]Rate constants ($k_{obs}$) at 1 mM dATP were calculated using the k_{pol} and K_d parameters listed above. [d]Single determination; all others were the average of two or more determinations.

misinsertion reactions. On the 13/19mer substrate, representing a generic DNA sequence not chosen for its hotspot or coldspot behavior, T-dGTP misinsertion by Pol ν is ~260-fold less efficient than that of Klenow fragment, and this counteracts the 6300-fold difference in the efficiency of correct (T-dATP) incorporation, resulting in ~24-fold lower selectivity of Pol ν against T-dGTP errors. By contrast, the kinetic parameters for G-dTTP misinsertion in the same sequence context are almost identical for the two enzymes, so that the entire 1000-fold difference in correct (G-dCTP) incorporation is manifested in a 1000-fold lower selectivity of Pol ν against G-dTTP errors, consistent with the abundance of these errors in synthesis by Pol ν. The similar kinetic parameters for G-dTTP misinsertion by Pol ν and Klenow fragment imply similar ground-state and transition-state energetics for this particular misinsertion in the Klenow fragment and Pol ν active sites, even though the energetics (and the corresponding kinetic parameters) of correct additions are substantially different.

Hotspot and Coldspot Sequences. The kinetic comparisons of the *lacZ* hotspot and coldspot sequences reveal that the efficiency of G-dTTP misinsertions by Pol ν varies over a range of nearly 100-fold. In contrast, the efficiency (k_{pol}/K_d) of correct G-dCTP insertions changes very little (~3-fold), though the individual k_{pol} and K_d values vary in interesting ways. Nucleotide binding is stabilized by more than 10-fold in the two hottest sequence contexts compared with the cold sequence. However, this does not contribute quantitatively to fidelity because the changes are similar in magnitude for both G-dCTP and G-dTTP insertions, indicating that ground-state binding of the ternary complex provides the same degree of selectivity against the G-dTTP nascent mispair at both hotspot and coldspot sequences. Instead, the important contributor to hotspot behavior is the rate constant, k_{pol}. On the hotspot DNA, k_{pol} is almost the same for correct and mismatched dNTPs, implying that the hotspot transition state fails to provide additional discrimination beyond what was already present in the ground state. In contrast, the coldspot substrate has ~15-fold faster k_{pol} for correct G-dCTP incorporation compared with G-dTTP misinsertion. Thus, the tighter substrate binding at the hotspot template position appears to correlate with a less optimal transition state for G-dCTP addition (slower reaction rate than at the coldspot). Conversely, correct G-dCTP incorporation on the coldspot template appears to use a weaker dNTP binding site and a more favorable transition state geometry, thus maintaining higher selectivity against the G-dTTP error. A similar correlation between tight dNTP binding and slow incorporation was observed in an earlier study of a Klenow fragment mutator mutant and attributed to altered active-site geometry.[44]

Sequence and Structural Implications. Compared to Klenow fragment, Pol ν exhibits stronger DNA binding, less efficient incorporation of correct base pairs, an active site favorable for G-dTTP nascent mispairs, and a strong influence of sequence context on the G-dTTP nascent mispair. Structural studies of Pol ν, which remain an elusive goal, will be essential for understanding differences between Klenow fragment and Pol ν and how they contribute to the kinetic properties reported here. In the absence of such information, sequence alignments of Pol ν with bacterial A-family DNA polymerases[51] and structural information about other A-family polymerases[23,52−54] suggest regions of Pol ν that may contribute to its unique properties. One feature that may be relevant to the DNA binding and processivity of Pol ν is a six-amino acid insertion predicted to be at the tip of the thumb subdomain, adjacent to conserved sequences already implicated in DNA binding in Klenow fragment.[55] A strong interaction with DNA may be necessary for Pol ν's proposed role in lesion bypass, especially when lesions compromise DNA interactions around the active site. Sequence alignments reveal that Pol ν also differs from more accurate A-family members in the O-helix (Figure 4), which makes several important interactions with the nascent base pair (Figure 4A).[9,25] One example is Lys679 of Pol ν, which aligns with Ala759 of Klenow fragment and Thr664 of Klentaq (Figure 4B). Changing Lys679 of Pol ν to the alanine or threonine present in the more accurate polymerases does indeed increase the fidelity of Pol ν.[51] Nonetheless, these changes did not alter the preferential formation of G-dTTP mismatches or the sequence dependence of Pol ν, indicating that such preferences depend on other enzyme−substrate interactions.

In a more global attempt to identify differences in the sequence of the O-helix of Pol ν that may affect specificity, we replaced residues in the O-helix of Klentaq with the corresponding sequence (residues 675−687, EQTKKVVYAVVYG) from Pol ν. The resulting chimera was active in gap-filling synthesis, but the accuracy of this reaction was much higher than that of Pol ν and similar to that of the parental Klentaq enzyme (data not shown). Further experiments (our unpublished data) targeted two additional regions in which Pol ν deviates from the A-family consensus (Figure 4). In the bacterial A-family polymerases, the N-terminus of the N-helix has the highly conserved D(I/V)H motif, where the histidine side chain interacts with the dNTP β-phosphate. The corresponding sequence is DVF in the Pol ν group. Mutation of Klenow fragment toward the Pol ν consensus (H734F) caused a substantial decrease in polymerase activity; however, the relative rates of T-dGTP versus G-dTTP misinsertions, and the selectivity against the G-dTTP mispair, were the same as in

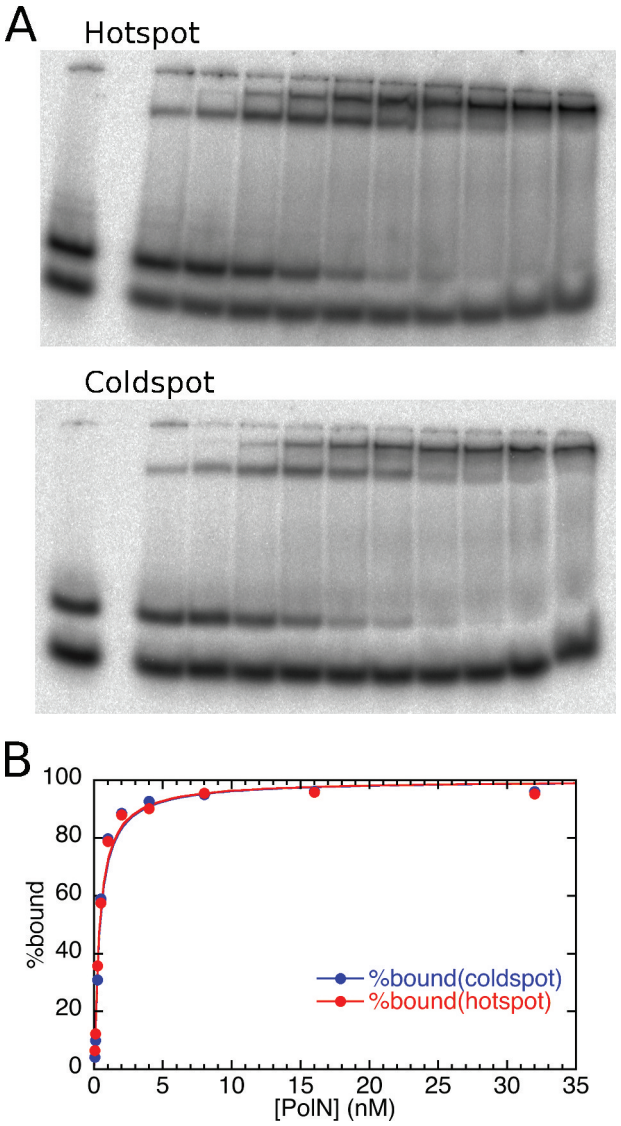

Figure 3. Gel mobility shift experiment comparing the binding of Pol ν-77 to a T-G mismatched DNA terminus in the context of the G(165) hotspot or the G(−66) coldspot sequence. (A) The labeled DNA was present at 0.025 nM; the leftmost lane of each gel shows the DNA in the absence of added protein, with excess primer strand having a mobility faster than that of the annealed duplex. Binding of the duplex is seen in the presence of Pol ν-77 at concentrations (from left to right) of 0.05, 0.1, 0.25, 0.5, 1, 2, 4, 8, 16, and 32 nM. (B) A plot of bound DNA vs Pol ν-77 concentration, fitted to a quadratic equation,[56] gave K_D values of 0.38 and 0.40 nM for the hotspot and coldspot sequences, respectively. Because only 23% of the Pol ν-77 was active, the true K_D is 0.1 nM.

wild-type Klenow fragment. A similar result was obtained by changing the N-terminus of the Klenow fragment Q-helix (motif 6 in ref 23) toward the Pol ν consensus (replacing residues 841−849 of Klenow fragment, RAAINAPMQ, with RQAINFVVQ). Although these experiments did not pinpoint a sequence motif responsible for the characteristic Pol ν error signature, they do suggest that the Klenow fragment and Klentaq active-site sequence motifs are optimized for efficiency, so that mutations away from the consensus tend to be associated with decreased polymerase activity. Pol ν, on the other hand, may have been fine-tuned by evolution for some specialized purpose for which maximal enzyme activity is not a priority. Similarly, the unusual error specificity of Pol ν and its particular DNA sequence specificities may be a consequence of the relaxed active-site specificity associated with its primary function within the cell.

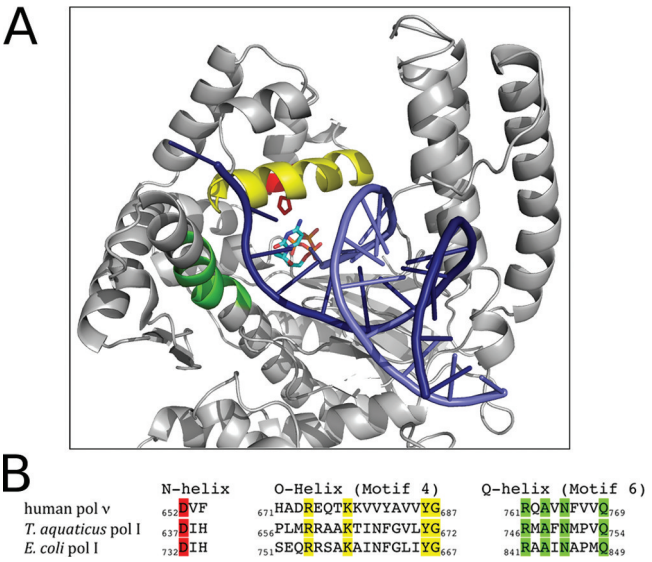

Figure 4. Regions of the A-family DNA polymerase structure where Pol ν shows interesting differences from the classical A-family conserved motifs. (A) The structure of the polymerase domain of the ternary (Pol−DNA−dNTP) complex of Klentaq (Protein Data Bank entry 3KTQ[54]). The protein structure is colored gray, with residues 501−523 at the tip of the thumb subdomain omitted to avoid obscuring the active-site region. The DNA duplex is colored blue, with the template strand darker, and the incoming dNTP is cyan with CPK coloring. Protein sequence motifs discussed in the text are colored as follows: red for the N-terminus of the N-helix (including the conserved histidine side chain), yellow for the O-helix, and green for the N-terminal portion of motif 6, within the Q-helix. (B) The alignment of the corresponding portions of sequence from human Pol ν, compared with Klenow fragment and Klentaq, representing the classical A-family DNA polymerases. The motif designations are from ref 23. Residues highly conserved in the alignment of both classical and Pol ν-type A-family DNA polymerases[51] are highlighted with the colors of the corresponding motifs in panel A.

■ ASSOCIATED CONTENT

Ⓢ Supporting Information

Additional gel mobility shift data for Pol ν (Figure S1). This material is available free of charge via the Internet at http://pubs.acs.org.

■ AUTHOR INFORMATION

Corresponding Author

*Department of Molecular Biophysics and Biochemistry, Yale University, Bass Center for Molecular and Structural Biology, 266 Whitney Avenue, P.O. Box 208114, New Haven, CT 06520-8114. Phone: (203) 432-8992. Fax: (203) 432-5175. E-mail: catherine.joyce@yale.edu.

Author Contributions

M.E.A. and O.P. contributed equally to this study.

Funding

This work was supported by Project Z01 ES065070 (to T.A.K.) from the Division of Intramural Research of the National Institute of Environmental Health Sciences, and National Institutes of Health Grant GM28550 (to C.M.J.).

■ ACKNOWLEDGMENTS

We thank Katarzyna Bebenek and Nigel Grindley for helpful comments on the manuscript, Komli Kofi Atsina and Ruoting (Valerie) Gong for kinetic data from Klenow fragment quoted in tables, and Christina Grindley for making the Pol ν-like Klenow fragment mutants.

■ ABBREVIATIONS

Pol, DNA polymerase; *Taq*, *Thermus aquaticus*; *Bst*, *Bacillus stearothermophilus*; Klentaq, portion of *Taq* DNA polymerase equivalent to Klenow fragment.

■ ADDITIONAL NOTE

[a]It is also possible that the hotspot for single deletions observed at G164 and G165 (Figure 1) results from a misinsertion−misalignment event initiated by a G-dTTP misinsertion at G(164), making the G-dTTP error rate at G(164) higher than that calculated from the observed base substitution mutations.

■ REFERENCES

(1) Bebenek, K., and Kunkel, T. A. (2004) Functions of DNA polymerases. *Adv. Protein Chem. 69*, 137−165.

(2) Marini, F., Kim, N., Schuffert, A., and Wood, R. D. (2003) POLN, a nuclear PolA family DNA polymerase homologous to the DNA cross-link sensitivity protein Mus308. *J. Biol. Chem. 278*, 32014−32019.

(3) Pang, M., McConnell, M., and Fisher, P. A. (2005) The *Drosophila mus308* gene product, implicated in tolerance of DNA interstrand crosslinks, is a nuclear protein found in both ovaries and embryos. *DNA Repair 4*, 971−982.

(4) Boyd, J. B., Sakaguchi, K., and Harris, P. V. (1990) *mus308* mutants of *Drosophila* exhibit hypersensitivity to DNA cross-linking agents and are defective in a deoxyribonuclease. *Genetics 125*, 813−819.

(5) Harris, P. V., Mazina, O. M., Leonhardt, E. A., Case, R. B., Boyd, J. B., and Burtis, K. C. (1996) Molecular cloning of *Drosophila mus308*, a gene involved in DNA cross-link repair with homology to prokaryotic DNA polymerase I genes. *Mol. Cell. Biol. 16*, 5764−5771.

(6) Zietlow, L., Smith, L. A., Bessho, M., and Bessho, T. (2009) Evidence for the involvement of human DNA polymerase N in the repair of DNA interstrand cross-links. *Biochemistry 48*, 11817−11824.

(7) Moldovan, G. L., Madhavan, M. V., Mirchandani, K. D., McCaffrey, R. M., Vinciguerra, P., and D'Andrea, A. D. (2010) DNA polymerase POLN participates in cross-link repair and homologous recombination. *Mol. Cell. Biol. 30*, 1088−1096.

(8) Yamanaka, K., Minko, I. G., Takata, K., Kolbanovskiy, A., Kozekov, I. D., Wood, R. D., Rizzo, C. J., and Lloyd, R. S. (2010) Novel enzymatic function of DNA polymerase ν in translesion DNA synthesis past major groove DNA-peptide and DNA-DNA cross-links. *Chem. Res. Toxicol. 23*, 689−695.

(9) Takata, K., Shimizu, T., Iwai, S., and Wood, R. D. (2006) Human DNA polymerase N (POLN) is a low fidelity enzyme capable of error-free bypass of 5*S*-thymine glycol. *J. Biol. Chem. 281*, 23445−23455.

(10) Bebenek, K., Joyce, C. M., Fitzgerald, M. P., and Kunkel, T. A. (1990) The fidelity of DNA synthesis catalyzed by derivatives of *Escherichia coli* DNA polymerase I. *J. Biol. Chem. 265*, 13878−13887.

(11) Donlin, M. J., Patel, S. S., and Johnson, K. A. (1991) Kinetic partitioning between the exonuclease and polymerase sites in DNA error correction. *Biochemistry 30*, 538−546.

(12) Kunkel, T. A., Patel, S. S., and Johnson, K. A. (1994) Error-prone replication of repeated DNA sequences by T7 DNA polymerase in the absence of its processivity subunit. *Proc. Natl. Acad. Sci. U.S.A. 91*, 6830−6834.

(13) Kunkel, T. A., and Soni, A. (1988) Exonucleolytic proofreading enhances the fidelity of DNA synthesis by chick embryo DNA polymerase-γ. *J. Biol. Chem. 263*, 4450−4459.

(14) Longley, M. J., Nguyen, D., Kunkel, T. A., and Copeland, W. C. (2001) The fidelity of human DNA polymerase γ with and without exonucleolytic proofreading and the p55 accessory subunit. *J. Biol. Chem. 276*, 38555−38562.

(15) Johnson, A. A., and Johnson, K. A. (2001) Exonuclease proofreading by human mitochondrial DNA polymerase. *J. Biol. Chem. 276*, 38097−38107.

(16) Kunkel, T. A. (2004) DNA replication fidelity. *J. Biol. Chem. 279*, 16895−16898.

(17) Kornberg, A., and Baker, T. A. (1992) *DNA Replication*, 2nd ed., W. H. Freeman and Co., New York.

(18) Tindall, K. R., and Kunkel, T. A. (1988) Fidelity of DNA synthesis by the *Thermus aquaticus* DNA polymerase. *Biochemistry 27*, 6008−6013.

(19) Eckert, K. A., and Kunkel, T. A. (1990) High fidelity DNA synthesis by the *Thermus aquaticus* DNA polymerase. *Nucleic Acids Res. 18*, 3739−3744.

(20) Kiefer, J. R., Mao, C., Hansen, C. J., Basehore, S. L., Hogrefe, H. H., Braman, J. C., and Beese, L. S. (1997) Crystal structure of a thermostable *Bacillus* DNA polymerase I large fragment at 2.1 Å resolution. *Structure 5*, 95−108.

(21) Johnson, S. J., and Beese, L. S. (2004) Structures of mismatch replication errors observed in a DNA polymerase. *Cell 116*, 803−816.

(22) Beard, W. A., and Wilson, S. H. (2001) DNA polymerases lose their grip. *Nat. Struct. Biol. 8*, 915−917.

(23) Patel, P. H., Suzuki, M., Adman, E., Shinkai, A., and Loeb, L. A. (2001) Prokaryotic DNA polymerase I: Evolution, structure, and "base flipping" mechanism for nucleotide selection. *J. Mol. Biol. 308*, 823−837.

(24) Arana, M. E., Seki, M., Wood, R. D., Rogozin, I. B., and Kunkel, T. A. (2008) Low-fidelity DNA synthesis by human DNA polymerase θ. *Nucleic Acids Res. 36*, 3847−3856.

(25) Arana, M. E., Takata, K., Garcia-Diaz, M., Wood, R. D., and Kunkel, T. A. (2007) A unique error signature for human DNA polymerase ν. *DNA Repair 6*, 213−223.

(26) Matsuda, T., Bebenek, K., Masutani, C., Rogozin, I. B., Hanaoka, F., and Kunkel, T. A. (2001) Error rate and specificity of human and murine DNA polymerase η. *J. Mol. Biol. 312*, 335−346.

(27) Rogozin, I. B., Pavlov, Y. I., Bebenek, K., Matsuda, T., and Kunkel, T. A. (2001) Somatic mutation hotspots correlate with DNA polymerase η error spectrum. *Nat. Immunol. 2*, 530−536.

(28) Gearhart, P. J., and Wood, R. D. (2001) Emerging links between hypermutation of antibody genes and DNA polymerases. *Nat. Rev. Immunol. 1*, 187−192.

(29) Pavlov, Y. I., Rogozin, I. B., Galkin, A. P., Aksenova, A. Y., Hanaoka, F., Rada, C., and Kunkel, T. A. (2002) Correlation of somatic hypermutation specificity and A-T base pair substitution errors by DNA polymerase η during copying of a mouse immunoglobulin κ light chain transgene. *Proc. Natl. Acad. Sci. U.S.A. 99*, 9954−9959.

(30) Pursell, Z. F., Isoz, I., Lundström, E. B., Johansson, E., and Kunkel, T. A. (2007) Yeast DNA polymerase ε participates in leading-strand DNA replication. *Science 317*, 127−130.

(31) Nick McElhinny, S. A., Stith, C. M., Burgers, P. M., and Kunkel, T. A. (2007) Inefficient proofreading and biased error rates during inaccurate DNA synthesis by a mutant derivative of *Saccharomyces cerevisiae* DNA polymerase δ. *J. Biol. Chem. 282*, 2324−2332.

(32) Nick McElhinny, S. A., Gordenin, D. A., Stith, C. M., Burgers, P. M., and Kunkel, T. A. (2008) Division of labor at the eukaryotic replication fork. *Mol. Cell 30*, 137−144.

(33) Beard, W. A., Shock, D. D., Vande Berg, B. J., and Wilson, S. H. (2002) Efficiency of correct nucleotide insertion governs DNA polymerase fidelity. *J. Biol. Chem. 277*, 47393−47398.

(34) Beard, W. A., and Wilson, S. H. (2003) Structural insights into the origins of DNA polymerase fidelity. *Structure 11*, 489−496.

(35) Bebenek, K., and Kunkel, T. A. (1995) Analyzing fidelity of DNA polymerases. *Methods Enzymol. 262*, 217−232.
(36) Arana, M. E., Powell, G. K., Edwards, L. L., Kunkel, T. A., and Petrovich, R. M. (2010) Refolding active human DNA polymerase ν from inclusion bodies. *Protein Expression Purif. 70*, 163−171.
(37) Joyce, C. M., and Derbyshire, V. (1995) Purification of *Escherichia coli* DNA polymerase I and Klenow fragment. *Methods Enzymol. 262*, 3−13.
(38) Joyce, C. M., Potapova, O., Delucia, A. M., Huang, X., Basu, V. P., and Grindley, N. D. F. (2008) Fingers-closing and other rapid conformational changes in DNA polymerase I (Klenow fragment) and their role in nucleotide selectivity. *Biochemistry 47*, 6103−6116.
(39) Astatke, M., Grindley, N. D. F., and Joyce, C. M. (1998) How *E. coli* DNA polymerase I (Klenow fragment) distinguishes between deoxy- and dideoxynucleotides. *J. Mol. Biol. 278*, 147−165.
(40) Johnson, K. A. (1995) Rapid quench kinetic analysis of polymerases, adenosinetriphosphatases, and enzyme intermediates. *Methods Enzymol. 249*, 38−61.
(41) Joyce, C. M. (2010) Techniques used to study the DNA polymerase reaction pathway. *Biochim. Biophys. Acta 1804*, 1032−1040.
(42) Eckert, K. A., and Kunkel, T. A. (1993) Effect of reaction pH on the fidelity and processivity of exonuclease-deficient Klenow polymerase. *J. Biol. Chem. 268*, 13462−13471.
(43) Bermek, O., Grindley, N. D. F., and Joyce, C. M. (2011) Distinct roles of the active-site Mg^{2+} ligands, Asp^{882} and Asp^{705}, of DNA polymerase I (Klenow fragment) during the prechemistry conformational transitions. *J. Biol. Chem. 286*, 3755−3766.
(44) Minnick, D. T., Liu, L., Grindley, N. D. F., Kunkel, T. A., and Joyce, C. M. (2002) Discrimination against purine-pyrimidine mispairs in the polymerase active site of DNA polymerase I: A structural explanation. *Proc. Natl. Acad. Sci. U.S.A. 99*, 1194−1199.
(45) Schaaper, R. M. (1993) Base selection, proofreading, and mismatch repair during DNA replication in *Escherichia coli*. *J. Biol. Chem. 268*, 23762−23765.
(46) Lee, H. R., and Johnson, K. A. (2006) Fidelity of the human mitochondrial DNA polymerase. *J. Biol. Chem. 281*, 36236−36240.
(47) Bebenek, K., Tissier, A., Frank, E. G., McDonald, J. P., Prasad, R., Wilson, S. H., Woodgate, R., and Kunkel, T. A. (2001) 5′-Deoxyribose phosphate lyase activity of human DNA polymerase ι in vitro. *Science 291*, 2156−2159.
(48) Kunkel, T. A., Hamatake, R. K., Motto-Fox, J., Fitzgerald, M. P., and Sugino, A. (1989) Fidelity of DNA polymerase I and the DNA polymerase I-DNA primase complex from *Saccharomyces cerevisiae*. *Mol. Cell. Biol. 9*, 4447−4458.
(49) Shcherbakova, P. V., Pavlov, Y. I., Chilkova, O., Rogozin, I. B., Johansson, E., and Kunkel, T. A. (2003) Unique error signature of the four-subunit yeast DNA polymerase ϵ. *J. Biol. Chem. 278*, 43770−43780.
(50) Fortune, J. M., Pavlov, Y. I., Welch, C. M., Johansson, E., Burgers, P. M., and Kunkel, T. A. (2005) *Saccharomyces cerevisiae* DNA polymerase δ: High fidelity for base substitutions but lower fidelity for single- and multi-base deletions. *J. Biol. Chem. 280*, 29980−29987.
(51) Takata, K. I., Arana, M. E., Seki, M., Kunkel, T. A., and Wood, R. D. (2010) Evolutionary conservation of residues in vertebrate DNA polymerase N conferring low fidelity and bypass activity. *Nucleic Acids Res. 38*, 3233−3244.
(52) Doublié, S., Tabor, S., Long, A. M., Richardson, C. C., and Ellenberger, T. (1998) Crystal structure of a bacteriophage T7 DNA replication complex at 2.2 Å resolution. *Nature 391*, 251−258.
(53) Johnson, S. J., Taylor, J. S., and Beese, L. S. (2003) Processive DNA synthesis observed in a polymerase crystal suggests a mechanism for the prevention of frameshift mutations. *Proc. Natl. Acad. Sci. U.S.A. 100*, 3895−3900.
(54) Li, Y., Korolev, S., and Waksman, G. (1998) Crystal structures of open and closed forms of binary and ternary complexes of the large fragment of *Thermus aquaticus* DNA polymerase I: Structural basis for nucleotide incorporation. *EMBO J. 17*, 7514−7525.
(55) Minnick, D. T., Astatke, M., Joyce, C. M., and Kunkel, T. A. (1996) A thumb subdomain mutant of the large fragment of *Escherichia coli* DNA polymerase I with reduced DNA binding affinity, processivity, and frameshift fidelity. *J. Biol. Chem. 271*, 24954−24961.
(56) Patel, S. S., Bandwar, R. P., and Levin, M. K. (2003) Transient-state kinetics and computational analysis of transcription initiation. In *Kinetic Analysis of Macromolecules* (Johnson, K. A., Ed.) pp 87−129, Oxford Univeristy Press, Oxford, U.K.